Extended test-particle method for predicting the inter- and intramolecular correlation functions of polymeric fluids

Yang-Xin Yu[a] and Jianzhong Wu[b]
Department of Chemical and Environmental Engineering, University of California, Riverside, California 92521-0425

(Received 21 October 2002; accepted 27 November 2002)

The Percus' test-particle method is extended to predict the inter- and intramolecular correlation functions of polymeric fluids using a density functional theory developed earlier [J. Chem. Phys. **117**, 2368 (2002)]. The calculated inter- and intramolecular distribution functions as well as the site–site correlation functions agree well with the results from Monte Carlo simulation for freely jointed hard-sphere chains. Compared with the integral-equation approaches and alternative density functional theories, the present method is free of molecular simulations as input and has the advantage of self-consistency among inter- and intramolecular correlation functions and thermodynamic properties. © *2003 American Institute of Physics.* [DOI: 10.1063/1.1539840]

I. INTRODUCTION

The conventional method for representing the microscopic structures of uniform polymeric fluids is from the polymer integral equation theory originally proposed by Chandler and Andersen for small rigid molecules,[1] and substantially expanded by Schweizer and co-workers for polymers.[2,3] Like the Ornstein–Zernike theory for monatomic fluids, the polymer integral equation theory formally connects the intramolecular correlation function with the intermolecular total and direct correlation functions of a polymeric fluid. The intramolecular correlation function describes the average configuration of a polymeric molecule that is, except for rigid molecules that have only one fixed configuration, coupled with the intermolecular total and direct correlation functions. For systems with known intramolecular correlation functions (e.g., small rigid molecules, polymer melts), the intermolecular total and direct correlation functions can be solved from the polymer integral equation theory conjugated with a suitable closure that defines an additional relation between total and direct correlation functions. There are at least two well-recognized difficulties on the application of the polymer integral-equation theory: First, it is often subtle to develop an appropriate closure for systems with both repulsive and attractive potentials and second, except for rigid molecules, self-consistency between inter- and intramolecular correlation functions is achieved through a complementary single-chain molecular simulation. Besides, the integral equation approach suffers inconsistency among different routes for thermodynamic properties and because calculation of thermodynamic variables requires reliable structural properties from low to high densities, the integral equation approach is often inconvenient for phase-diagram calculations. Nevertheless, polymer integral equation theory has been successfully applied to describing the microscopic structures of a broad variety of polymeric systems, including solutions of flexible and semiflexible polymers, polyelectrolytes, polymer melts, block copolymers, and liquid crystals.[4]

An alternative approach for representing both structural and thermodynamic properties of polymeric fluids was based on chemical equilibrium proposed by Chandler and Pratt,[5,6] and along similar lines, by Wertheim.[7,8] The equivalence of the theory by Chandler and Pratt and the thermodynamic perturbation theory (TPT) by Wertheim was demonstrated by Kierlik and Rosinberg before.[9,10] In this alternative approach, a polymeric system is represented as an effective associating system of monomers where in the limit of complete association, the original polymer chains can be formed by chemical reactions. The excess Helmholtz energy due to the polymerization (or chain formation) is related to the association equilibrium through the multibody cavity correlation functions of the monomeric fluid.[11–14] The polymerization approach gives self-contained structural and thermodynamic properties and employs no molecular simulations as input.[9,10] While this approach provides reasonable thermodynamic properties and intermolecular correlation functions, it is unable to predict the nonideal behavior of intramolecular correlation functions of polymeric fluids.[9,10] Recently, Stell and co-workers[15–17] proposed a product-reactant Ornstein–Zernike approach (PROZA) based on Wertheim's thermodynamic perturbation theory and polymer Percus–Yevick closure. PROZA yields analytical expressions for the average monomer–monomer radial distribution functions and the compressibility of polymeric fluids that both are in good agreement with simulation results. Similar approaches based on Wertheim's theory have been used by other groups.[18–24] As in Wertheim's original theory, all polymerization-based integral equation theories fail to represent the nonideal behavior of the intramolecular correlation functions.

As proposed long ago by Percus,[25] the structure of a uniform fluid can be represented by the local inhomogeneity

[a]Also at the Department of Chemical Engineering, Tsinghua University, Beijing 100084, People's Republic of China.
[b]Author to whom correspondence should be addressed. Electronic mail: jwu@engr.ucr.edu

of density distributions around an arbitrarily fixed particle. Percus' method was recently used by Yethiraj and coworkers to investigate the intermolecular correlation functions of tangentially connected and fused hard-sphere chains.[26] While the test-particle method is convenient for calculating the radial distribution functions of monatomic fluids, its application for polymers involves a complicated external field that depends on the positions of all fixed segments. As a result, the site–site correlation functions can only be calculated in couple with a two-molecule simulation.[26]

In this work, we extend Percus' test-particle method for polymeric fluids and investigate the inter- and intramolecular correlation functions as well as the site–site distribution functions using a density-functional theory proposed earlier.[27] Different from the test-particle method used by Yethiraj and co-workers,[26] only one segment (instead of the entire polymer chain) is fixed and the segment-segment correlation functions are directly calculated from the density distributions of segments from the tethered polymer chain and those from the free chains. This extended test-particle method avoids molecular simulations as input and provides both intra- and intermolecular correlation functions directly. Although this work concerns only the freely jointed hard-sphere chains as the model system, a similar approach should be applicable to systems with more realistic potentials.

II. TEST-PARTICLE METHOD FOR POLYMERIC FLUIDS

Many years ago Percus suggested that the radial distribution functions of a uniform fluid could be obtained from the density profiles around a test molecule fixed at the origin. Percus' idea provides a convenient way to derive the closure equations for the integral-equation theory of monatomic fluids and more important, self-consistent structural properties of uniform systems by using a density-functional theory. While the application of Percus' method for simple fluids is relatively straightforward,[28] calculation of the local density distributions of a polymeric fluid is more difficult because if one molecule that contains multiple segments is fixed at the origin, the external field on the ''free'' molecules depends on the configuration of the fixed molecule. As a result, the site–site intermolecular correlation functions can only be calculated through a complementary Monte Carlo simulation.[26] However, if only one segment from a polymeric molecule is fixed at the origin, the distributions of other segments from the tethered molecule as well as the segments from the free molecules can be calculated simultaneously by minimization of the grand potential. As for monatomic fluids, these distribution functions are directly related to the inter- and intramolecular correlation functions of the polymeric fluid. Compared with the scenario where an entire molecule is fixed, one obvious advantage of this method is that the external field for calculating the density distributions is spherically symmetric. Moreover, this method avoids the ensemble averages over all configurations of the fixed molecule and thereby eliminating extra molecular simulations.

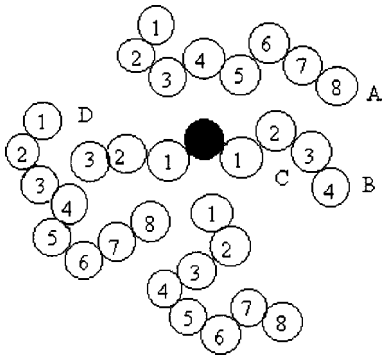

FIG. 1. A schematic representation of the extended test-particle method for polymeric fluids. Here a middle segment from a hard-sphere 8-mer (filled circle) is fixed at the origin. The density distributions of segments from the tethered fragments (B&D) and the free molecules (A) are related to the intra- and intermolecular segment–segment correlation functions.

To fix the idea, we consider the microscopic structure of a model polymeric fluid consisting of tangentially connected hard-sphere chains (Fig. 1). Suppose that one segment from an arbitrarily selected chain is fixed at the origin. The segments of free molecules, designated as *A*, are sequentially ranked along the backbone while the tethered molecule, designated as *B*, is distinguished from the free molecules by separating into two fragments at the fixed point. These two fragments, also sequentially ranked, are labeled as *C* and *D*, respectively.

At equilibrium, the density distributions of free chains and the tethered fragments satisfy the variational relations,

$$\frac{\delta\Omega}{\delta\rho^{(A)}(\mathbf{R}^{(A)})}=\frac{\delta\Omega}{\delta\rho^{(C)}(\mathbf{R}^{(C)})}=\frac{\delta\Omega}{\delta\rho^{(D)}(\mathbf{R}^{(D)})}=0, \tag{1}$$

where Ω stands for the grand potential functional, $\rho^{(l)}(\mathbf{R}^{(l)})$, $l=A$, C, and D, are density profiles, and $\mathbf{R}^{(l)}=\{r_1^{(l)},r_2^{(l)},\ldots,r_{M_l}^{(l)}\}$ is a composite vector that specifies the positions of M_l segments of chain l. The grand potential functional for determining density profiles must be supplied by an adequate density-functional theory for the polymeric system.

The segmental distributions of the free molecules around the fixed segment is related to the intermolecular site–site correlation functions,

$$g_{ij}(r)=\rho_{si,j}^{(A)}(r)/\rho_A, \tag{2}$$

where $\rho_{si,j}^{(A)}(r)$ is the density profile of segment i on the free molecules around the fixed segment j, and ρ_A is the bulk density of segment i. Because all segments along the polymeric chain are distinguishable, ρ_A is the same as the bulk molecular density. Similarly, the distributions of the segments from fragments *C* and *D* are directly related to the intramolecular correlation functions,

$$w_{ij}(r)=\rho_{si,j}^{(B)}(r), \tag{3}$$

where $\rho_{si,j}^{(B)}(r)$ is the density of segment i from the tethered chain *B*. Because there is only one tethered polymer chain, the segmental densities of chain *B* satisfy the normalization condition,

$$\int \rho^{B}_{si,j}(r)d\mathbf{r}=1. \tag{4}$$

The site–site inter- and intramolecular correlation functions specify all detail microscopic structures of a polymeric fluid. In principle, all these functions can be determined from a density functional theory. From the site–site correlation functions, we can calculate the average intermolecular correlation function from

$$g(r)=\frac{1}{M_A^2}\sum_{i=1}^{M_A}\sum_{j=1}^{M_A} g_{ij}(r) \tag{5}$$

and the average intramolecular correlation functions from

$$w(r)=\frac{1}{M_A}\sum_{i=1}^{M_A}\sum_{j=1}^{M_A} w_{ij}(r), \tag{6}$$

where M_A is the number of segments at each free molecule A. Average molecular correlation functions are often sufficient to specific the local structures of homopolymers.

III. DENSITY FUNCTIONAL THEORY

The system considered above is equivalent to a mixture of three polymeric components $(A+C+D)$ in a spherically symmetric external field due to the fixed segment. The density functional theory for inhomogeneous polymeric fluids has been reported before.[27] Briefly, the grand potential functional Ω is related to the Helmholtz energy functional F via a Legendre transform,

$$\Omega=F[\rho^{(A)}(\mathbf{R}^{(A)}),\rho^{(C)}(\mathbf{R}^{(C)}),\rho^{(D)}(\mathbf{R}^{(D)})] + \sum_{l=A,C,D}\int [\Psi^{(l)}(\mathbf{R}^{(l)})-\mu_l]\rho^{(l)}(\mathbf{R}^{(l)})d\mathbf{R}^{(l)}, \tag{7}$$

where $d\mathbf{R}^{(l)}=d\mathbf{r}_1^{(l)}d\mathbf{r}_2^{(l)}\cdots d\mathbf{r}_{M_l}^{(l)}$ represents a set of differential volumes for the polymer chain l of M_l segments, μ_l is the polymer chemical potential, and $\Psi^{(l)}(\mathbf{R}^{(l)})$ denotes the total external potential on chain l. The total external potential on each molecule is equal to the sum of the potential energy on its individual segments $\Psi^{(l)}(\mathbf{R}^{(l)})=\Sigma_{i=1}^{M_l}\varphi_i^{(l)}(\mathbf{r}_i^{(l)})$. For any segment that is not immediately bonded with the fixed segment, the external potential is identical to the segment–segment interaction energy, while for the two segments that are directly connected to the fixed segment, the external potential includes also the bonding energy. For tangentially connected hard-sphere chains that are considered in this work, the bonding potential, v_b, is given by

$$\exp[-\beta v_b(\mathbf{r}_i,\mathbf{r}_j)]=\frac{\delta(|r_i-r_j|-\sigma)}{4\pi\sigma^2}, \tag{8}$$

where segments i and j are nearest neighbors from the same molecule, β^{-1} is the Boltzmann's constant k_B multiplied by the thermal temperature T, and $\delta(r)$ is the Dirac delta function.

The Helmholtz energy functional F can be formally expressed as an ideal-gas contribution F_{id} plus an excess term F_{ex} that accounts for intra- and intermolecular interactions (other than the bonding potentials),

$$F=F_{\mathrm{id}}+F_{\mathrm{ex}}. \tag{9}$$

The ideal-gas contribution to the Helmholtz energy functional is exactly known

$$\beta F_{\mathrm{id}}=\sum_{l=A,C,D}\int d\mathbf{R}^{(l)}\rho^{(l)}(\mathbf{R}^{(l)})[\ln\rho^{(l)}(\mathbf{R}^{(l)})-1] + \beta\sum_{l=A,C,D}\int d\mathbf{R}^{(l)}\rho^{(l)}(\mathbf{R}^{(l)})V_b^{(l)}(\mathbf{R}^{(l)}), \tag{10}$$

where the total bonding potential for a chain l is

$$V_b^{(l)}(\mathbf{R}^{(l)})=\sum_{i=1}^{M_l-1} v_b(\mathbf{r}_i,\mathbf{r}_{i+1}). \tag{11}$$

Because of the bonding potentials on the right-hand side of Eq. (10), the Helmholtz energy functional for a polymeric ideal-gas mixture is different from that for a monatomic ideal gas. However, Eq. (10) does not take into account the intramolecular interactions other than the direct chain connectivity.

To derive the excess Helmholtz energy functional due to both intra- and intermolecular interactions beyond the chain connectivity, we incorporate a modification of the fundamental-measure theory (FMT) developed recently[28] with the polymerization theory of Chandler and Pratt,[5,6] and Wertheim[8]

$$\beta F_{\mathrm{ex}}=\int d\mathbf{r}\{\Phi^{\mathrm{hs}}[n_\alpha(\mathbf{r})]+\Phi^{\mathrm{chain}}[n_\alpha(\mathbf{r})]\}, \tag{12}$$

where $\Phi^{\mathrm{hs}}[n_\alpha(\mathbf{r})]$ and $\Phi^{\mathrm{chain}}[n_\alpha(\mathbf{r})]$ are, respectively, the reduced excess Helmholtz energy densities due to hard-sphere repulsion and chain connectivity. Different from the direct bonding potential, the chain connectivity term arises from the indirect interactions due to the exclude volume of individual segments. In writing Eq. (12), we assume that the excess Helmholtz energy functional due to chain connectivity can be effectively accounted using only segmental densities.

As in the original FMT, the scalar and vector weighted densities are defined as

$$n_\alpha(\mathbf{r})=\sum_l n_{\alpha l}(\mathbf{r})=\sum_l\int\rho^{(l)}(\mathbf{r}')w_l^{(\alpha)}(\mathbf{r}-\mathbf{r}')d\mathbf{r}', \tag{13}$$

where the subscripts $\alpha=0$, 1, 2, 3, $V1$, $V2$ denote the index of six weight functions $w_l^{(\alpha)}(r)$ that characterize the volume, surface area, and surface vector of a spherical particle. The total segmental density of chain l, $\rho^{(l)}(\mathbf{r})$, is given by a sum of that for individual segments,

$$\rho^{(l)}(\mathbf{r})=\sum_{i=1}^{M_l}\rho_{si}^{(l)}(\mathbf{r})=\sum_{i=1}^{M_l}\int d\mathbf{R}^{(l)}\delta(\mathbf{r}-\mathbf{r}_i^{(l)})\rho^{(l)}(\mathbf{R}^{(l)}), \tag{14}$$

where $\rho_{si}^{(l)}(\mathbf{r})$ stands for the local density of segment i from chain l.

All weight functions are independent of the density profiles. Among them, three weight functions are directly related to the geometry of a spherical particle of diameter σ,

$$w_l^{(2)}(r)=\delta(\sigma/2-r), \tag{15}$$

$$w_l^{(3)}(r)=\Theta(\sigma/2-r), \tag{16}$$

$$\mathbf{w}_l^{(V2)}(\mathbf{r})=(\mathbf{r}/r)\,\delta(\sigma/2-r), \tag{17}$$

where $\Theta(r)$ is the Heaviside step function, and $\delta(r)$ denotes the Dirac delta function. Integration of the two scalar functions, $w_l^{(2)}(r)$ and $w_l^{(3)}(r)$, with respect to the position gives the particle surface area and volume, respectively, and integration of the vector function $\mathbf{w}_l^{(V2)}(\mathbf{r})$ is related to the gradient across a sphere in the $\mathbf{r}$ direction. Other weight functions are proportional to the three geometric functions given in Eqs. (15)–(17),

$$w_l^{(0)}(r)=\frac{w_l^{(2)}(r)}{\pi\sigma^2};\quad w_l^{(1)}(r)=\frac{w_l^{(2)}(r)}{2\pi\sigma};$$
$$\mathbf{w}_l^{(V1)}(\mathbf{r})=\frac{\mathbf{w}_l^{(V2)}(\mathbf{r})}{2\pi\sigma}. \tag{18}$$

As in our previous work,[28] the hard-sphere Helmholtz energy density consists of contributions from scalar weighted densities and vector weighted densities,

$$\Phi^{\mathrm{hs}}\{n_\alpha(\mathbf{r})\}=\Phi^{\mathrm{hs}(S)}\{n_\alpha(\mathbf{r})\}+\Phi^{\mathrm{hs}(V)}\{n_\alpha(\mathbf{r})\}, \tag{19a}$$

where the superscripts (S) and (V) stand for contributions from scalar and vector weighted densities, respectively, given by

$$\Phi^{\mathrm{hs}(S)}\{n_\alpha(\mathbf{r})\}=-n_0\ln(1-n_3)+\frac{n_1n_2}{1-n_3}+\frac{n_2^3}{36\pi n_3^2}\times\ln(1-n_3)+\frac{n_2^3}{36\pi n_3(1-n_3)^2}, \tag{19b}$$

$$\Phi^{\mathrm{hs}(V)}\{n_\alpha(\mathbf{r})\}=-\frac{\mathbf{n}_{V1}\cdot\mathbf{n}_{V2}}{1-n_3}-\frac{n_2\mathbf{n}_{V2}\cdot\mathbf{n}_{V2}}{12\pi n_3^2}\ln(1-n_3)-\frac{n_2\mathbf{n}_{V2}\cdot\mathbf{n}_{V2}}{12\pi n_3(1-n_3)^2}. \tag{19c}$$

In the limit of a bulk fluid, the two vector weighted densities $\mathbf{n}_{V1}$ and $\mathbf{n}_{V2}$ vanish, and the Helmholtz energy functional becomes identical to that from the Boublik–Mansoori–Carnahan–Starling–Leland (BMCSL) equation of state.[29,30] The Helmholtz energy density due to chain formation at an inhomogeneous condition is given by[27]

$$\Phi^{\mathrm{chain}}(n_\alpha)=\frac{1-M_A}{M_A}n_{0A}\zeta_A\ln y_{11}^{\mathrm{hs}}(\sigma,n_\alpha)+\sum_{l=C,D}n_{0l}\zeta_l\ln y_{11}^{\mathrm{hs}}(\sigma,n_\alpha), \tag{20}$$

where $\zeta_l=1-\mathbf{n}_{V2l}\cdot\mathbf{n}_{V2l}/n_{2l}^2$ and $y_{11}^{\mathrm{hs}}(\sigma,n_\alpha)$ is the contact value of the cavity correlation between segments and can be expressed as

$$y_{11}^{\mathrm{hs}}(\sigma,n_\alpha)=\frac{1}{1-n_3}+\frac{n_2\sigma\zeta}{4(1-n_3)^2}+\frac{n_2^2\sigma^2\zeta}{72(1-n_3)^3}, \tag{21}$$

where $\zeta=1-\mathbf{n}_{V2}\cdot\mathbf{n}_{V2}/n_2^2$.

Minimization of the grand potential with respect to the density profiles of free molecules and the polymeric fragments yields the following Euler–Lagrange equations,

$$\rho^{(l)}(\mathbf{R}^{(l)})=\exp[\beta\mu_l-\beta V_b^{(l)}(\mathbf{R}^{(l)})-\beta\Psi^{(l)}(\mathbf{R}^{(l)})-\beta\Lambda^{(l)}(\mathbf{R}^{(l)})]\quad(l=A,C,D), \tag{22}$$

where $\Lambda^{(l)}(\mathbf{R}^{(l)})=\delta F_{\mathrm{ex}}/\delta\rho^{(l)}(\mathbf{R}^{(l)})$ represents an effective potential field due to intra- and intermolecular interactions. Because the excess Helmholtz energy functional depends only on the density distributions of individual segments, the effective potential can be simplified to

$$\Lambda^{(l)}(\mathbf{R}^{(l)})=\frac{\delta F_{\mathrm{ex}}}{\delta\rho^{(l)}(\mathbf{R}^{(l)})}=\sum_{i=1}^{M_l}\frac{\delta F_{\mathrm{ex}}}{\delta\rho^{(l)}(\mathbf{r}_i^{(l)})}. \tag{23}$$

Substituting Eq. (23) into Eq. (22) yields

$$\rho^{(l)}(\mathbf{R}^{(l)})=\exp\left\{\beta\mu_l-\beta V_b^{(l)}(\mathbf{R}^{(l)})-\beta\sum_{i=1}^{M_l}\lambda_i^{(l)}(\mathbf{r}_i^{(l)})\right\}, \tag{24a}$$

where $\lambda_i^{(l)}(\mathbf{r}_i^{(l)})$ is related to the excess Helmholtz energy F_{ex} and the external potential $\varphi_i^{(l)}(\mathbf{r}_i^{(l)})$ by

$$\lambda_i^{(l)}(\mathbf{r}_i^{(l)})=\frac{\delta F_{\mathrm{ex}}}{\delta\rho^{(l)}(\mathbf{r}_i^{(l)})}+\varphi_i^{(l)}(\mathbf{r}_i^{(l)}). \tag{24b}$$

Equation (24) indicates that as in a typical self-consistent-field theory, the segment density is determined by the chain connectivity and an effective external potential $\lambda_i^{(l)}(\mathbf{r}_i^{(l)})$. Because Eq. (23) involves only the total segmental density, the self-consistent field is identical for all segments.

Introducing the segmental densities $\rho_{si}^{(l)}(\mathbf{r})$ into Eq. (24) yields a set of coupled integral equations,

$$\rho_{si}^{(l)}(\mathbf{r})=\int d\mathbf{R}^{(l)}\delta(\mathbf{r}-\mathbf{r}_i^{(l)})\exp\left[\beta\mu_l-\beta V_b^{(l)}(\mathbf{R}^{(l)})-\beta\sum_{j=1}^{M_l}\lambda_j^{(l)}(\mathbf{r}_j^{(l)})\right]. \tag{25}$$

Substitution of Eq. (25) into Eq. (14) gives the average segmental density of chain molecules

$$\rho^{(l)}(\mathbf{r})=\exp(\beta\mu_l)\int d\mathbf{R}^{(l)}\sum_{i=1}^{M_l}\delta(\mathbf{r}-\mathbf{r}_i^{(l)})\times\exp\left[-\beta V_b^{(l)}(\mathbf{R}^{(l)})-\beta\sum_{j=1}^{M_l}\lambda_j^{(l)}(\mathbf{r}_j^{(l)})\right]. \tag{26}$$

Equation (26) represents the key equation of this work.

IV. NUMERICAL METHOD

Because of the spherical symmetry, the density distributions of both free and tethered segments vary only in the radial direction. As a result, the total density profile can be expressed as

$$\rho^{(l)}(\mathbf{r})=\rho^{(l)}(r). \tag{27}$$

Subsequently, Eq. (26) can be simplified to[27]

$$\rho_{si}^{(l)}(r)=\exp(\beta\mu_l)\exp[-\beta\lambda_i^{(l)}(r)]G_L^{(l)i}(r)G_R^{(l)i}(r) \quad (l=A,C,D). \tag{28}$$

In Eq. (28), $G_L^{(A)i}(r)$ is the Green function for $l=A$ (free molecule), which is determined from the recurrence relation,

$$G_L^{(A)i}(r)=\int dr'\exp[-\beta\lambda_i^{(A)}(r')]\times\frac{r'\theta(\sigma-|r'-r|)}{2\sigma r}G_L^{(A)i-1}(r') \tag{29}$$

for $i=2,...,M_A$ with $G_L^{(A)1}(r)=1$. Because the external potential is the same for all the monomers on the chain A, we have the additional symmetric relations

$$G_R^{(A)M-i+1}=G_L^{(A)i}. \tag{30}$$

For $l=C$ and D, the density profiles of the two immediate neighbors of the fixed segment are given by

$$\rho_{s1}^{(C)}=\rho_{s1}^{(D)}=\frac{\delta(r-\sigma)}{4\pi\sigma^2}. \tag{31}$$

The Green function for the next immediate neighbors is determined from

$$G_L^{(l)2}(r)=\exp[-\beta\lambda_2^{(l)}(\sigma)]\frac{\theta(\sigma-|r-\sigma|)}{2r} \tag{32}$$

and those for the remaining segments are determined from the iteration

$$G_L^{(l)i}(r)=\int dr'\exp[-\beta\lambda_i^{(l)}(r')]\times\frac{r'\theta(\sigma-|r-r'|)}{2\sigma r}G_L^{(l)i-1}(r') \tag{33}$$

for $i=3,...,M_l$. The function $G_R^{(l)i}(r)$ is calculated from the recurrence relation,

$$G_R^{(l)i}(r)=\int dr'\exp[-\beta\lambda_i^{(l)}(r')]\times\frac{r\theta(\sigma-|r'-r|)}{2\sigma r'}G_R^{(l)i+1}(r') \tag{34}$$

with $G_R^{(l)M_l}(r)=1$.

The chemical potentials for solving the density profiles are obtained directly from Wertheim's TPT1 equation of state for bulk hard-sphere-chain fluids[31]

$$\beta\mu_A=\ln\rho_A+M_A\beta\mu_A^{\mathrm{hs}}(\rho_b)+(1-M_A)\left[\ln y_{11}^{\mathrm{hs},b}(\sigma)+\rho_b\frac{\partial\ln y_{11}^{\mathrm{hs},b}(\sigma)}{\partial\rho_b}\right], \tag{35}$$

where $\rho_b=M_A\rho_A$ is the bulk densities of segments, μ_A^{hs} is the excess chemical potential of corresponding hard spheres given by the Carnahan–Starling equation of state.[32] Equation (35) is identical to Eq. (26) in the absence of the external potential. The chemical potentials of the fragments C and D are determined by the normalization conditions $\int 4\pi r^2\rho_{si}^{(C)}(r)dr=1$, where $i=2,3,...,M_C$, and $\int 4\pi r^2\rho_{si}^{(D)}(r)dr=1$, where $i=2,3,...,M_D$.

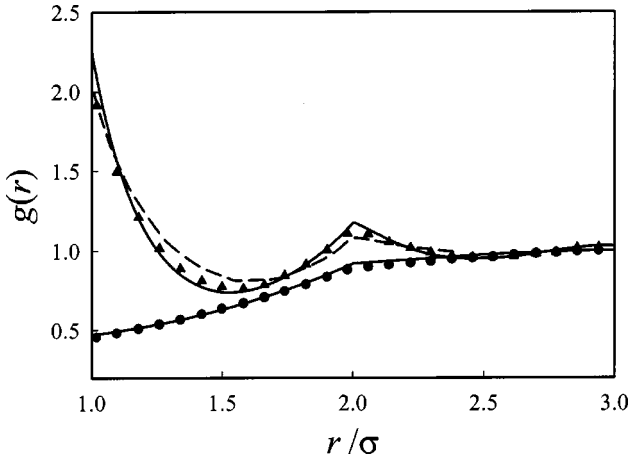

FIG. 2. The average intermolecular radial distribution functions of hard-sphere 4-mers at packing fractions $\eta=0.1$ (solid circles) and 0.4 (solid triangles). The solid lines are calculated from this work, the dashed lines are from an alternative density functional theory proposed by Yethiraj *et al.*, and the symbols are from molecular simulation (Ref. 26).

In calculating the inter- and intramolecular correlation functions, we fix the segments of a polymer chain one by one and the density distributions around the fixed segment are calculated with Eqs. (28)–(34). Because of symmetry, $M_A/2$ (if M_A is even) or $(M_A+1)/2$ (if M_A is odd) calculations are required for predicting the detail local structures of homopolymers consisting of M_A identical segments. While the amount of calculations would be substantial for long polymers, we can simplify the procedure by calculating the correlation functions only related to end and middle segments because in a long polymer chain, the site–site correlation functions of other segments are expected to be similar to those for the middle segments. The density profiles are solved using the Picard-type iterative method. The iteration starts with bulk densities as initial guess, the effective fields $\lambda_i^{(l)}(r)$, the Green functions $G_R^{(l)i}(r)$ and $G_L^{(l)i}(r)$ are then calculated with the recurrence relations Eqs. (29)–(34). Subsequently, a set of new density profiles are obtained from Eq. (28), which are then mixed with the previous results as new input. The iteration repeats until the percentage change is smaller than 0.01 at all points. The numerical integrations are performed using the trapezoidal rule with the step size $\Delta r=0.02\sigma$.

V. RESULTS AND DISCUSSION

We have calculated the inter- and intramolecular radial distribution functions for freely jointed hard-sphere 4-mers, 8-mers, and 20-mers. Figure 2 compares the calculated intermolecular correlation functions with the Monte Carlo simulation data for hard-sphere 4-mers at two packing fractions $\eta=0.1$ and 0.4. Here the overall packing fraction η is defined as $\eta=\pi\rho\sigma^3/6$, where ρ is the number density of segments. Also shown in Fig. 2 are the theoretical predictions using an alternative density functional theory based on the original Percus' test-particle method.[26] While both approaches predict

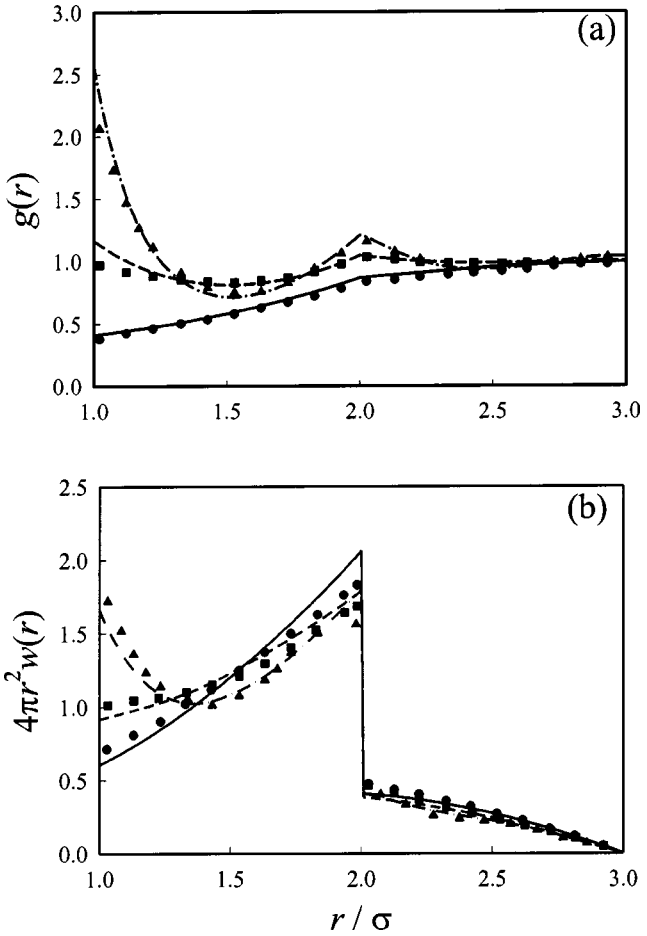

FIG. 3. The average correlation functions of freely jointed hard-sphere 4-mers: (a) intermolecular correlation functions, and (b) nonbonded intramolecular correlation functions. The symbols are the simulation values (Ref. 23) and curves are from the present theory. The overall packing fractions are η=0.0524 (circles and solid lines), 0.2618 (squares and dashed lines), and 0.4189 (triangles and dotted–dashed lines).

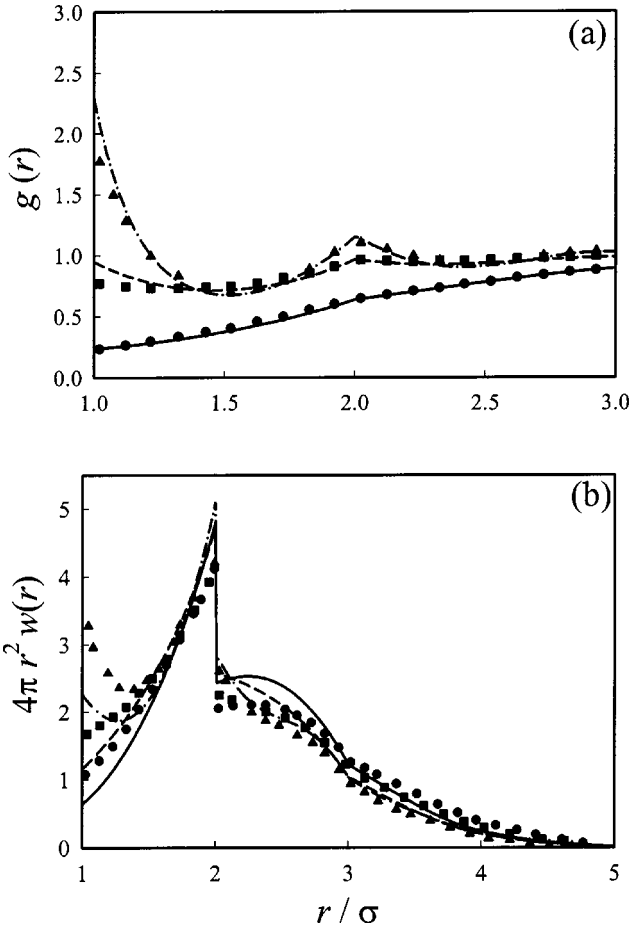

FIG. 4. Same as in Fig. 3 but for 8-mers.

intermolecular correlation functions in good agreement with simulation results, one significant advantage of the present approach is free of two-molecular simulations for intermolecular structures.

Figures 3–5 compare theoretical predictions with the Monte Carlo simulation data by Chang and Sandler,[23] and by Yethiraj[33] for hard-sphere 4-mers, 8-mers, and 20-mers. The depletion of intermolecular segments at low density is due to the chain connectivity while the opposite trend at high density is due to the packing effect. Except the contact values, our method gives accurate intermolecular correlation functions including the cusp at $r=2\sigma$ related to the fixed bond length. In general, the theoretical predictions are in good agreement with the simulation results at both high and low densities. However, the theory overestimates the intermolecular radial distribution functions and underestimates the intramolecular radial distribution function near contact as the chain length increases. For the systems considered in this work, the present theory provides slightly more accurate intermolecular correlation functions than Wertheim's multidensity integral-equation theory,[8,21,23] especially for long chains at low densities.

Figures 3(b)–5(b) present the average nonbonded intramolecular radial distribution functions $4\pi r^2 w(r)$. The discontinuity at $r=2\sigma$ is due to the direct interaction between next nearest neighbors along the polymer chain. For $r<2\sigma$, the intramolecular correlation function increases monotonically with separation at low density. However, it shows a minimum at approximately $r=1.5\sigma$ as density increases. For $r>2\sigma$, our theory reproduces the essential features of nonmonotonic decaying of the intramolecular correlations. While the intramolecular correlation functions predicted from the present theory improves significantly in comparison with alternative approaches in the literature, the agreement between theory and simulation is only semiquantitative, especially at contact values. The discrepancy is likely related to the approximation in representing the excess Helmholtz energy functional due to the chain connectivity (where only two-body correlation functions are used). When a segment is fixed at the origin, the intramolecular correlation functions are sensitive to multibody correlations among the segments belonging to the same molecule.

Finally, Fig. 6 shows the intermolecular site–site radial distribution functions predicted from the present density functional theory and those from the Monte Carlo simulation[34] for freely jointed hard-sphere 4-mers. Our theory gives accurate end–end segment radial distribution functions at the entire density region, however it overpredicts the end–middle and middle–middle segment radial distribution functions near contact. In Fig. 7, we compare the theo-

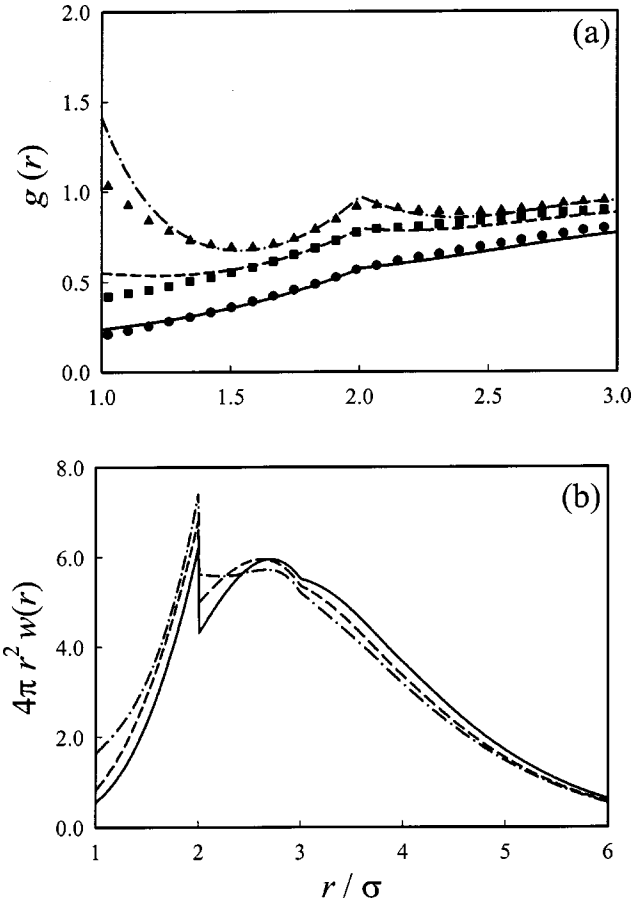

FIG. 5. The average correlation functions of freely jointed hard-sphere 20-mers: (a) intermolecular correlation functions, and (b) nonbonded intramolecular correlation functions. The symbols are the simulation values (Ref. 33) and curves are from the present theory. The overall packing fractions are η=0.1 (circles and solid lines), 0.2 (squares and dashed lines), and 0.35 (triangles and dotted–dashed lines).

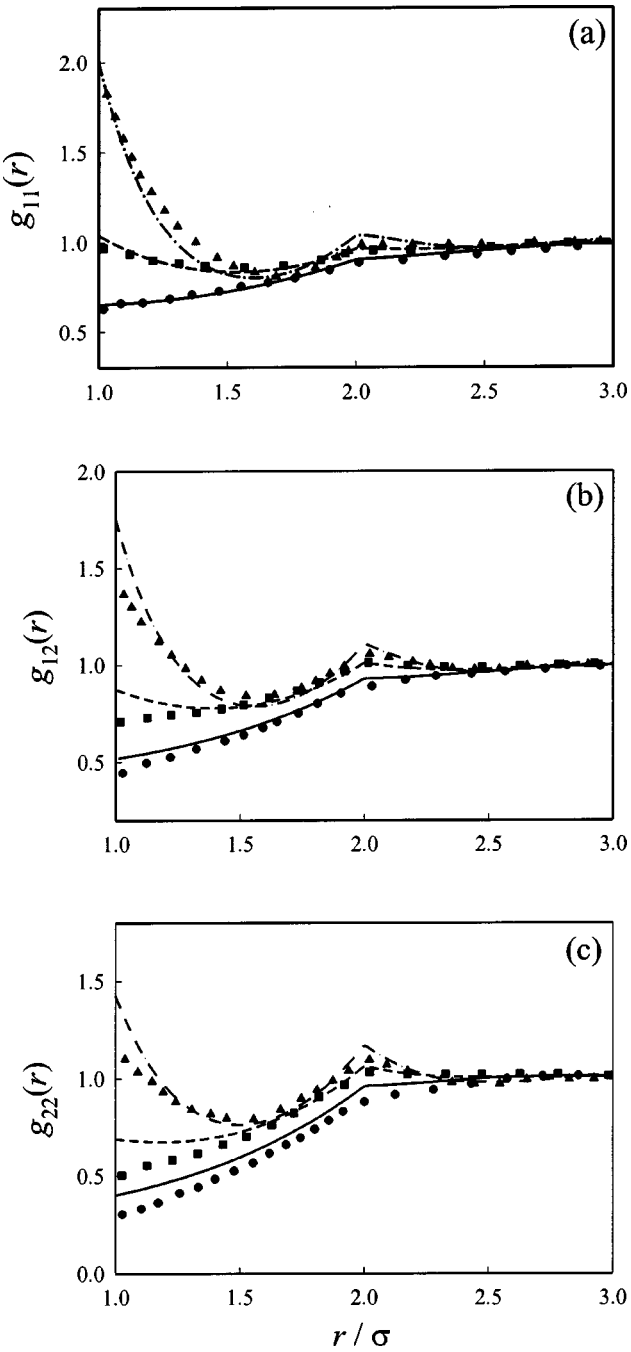

FIG. 6. Intermolecular site–site distribution functions of freely jointed hard-sphere 4-mers: (a) $g_{11}(r)$, (b) $g_{12}(r)$, and (c) $g_{22}(r)$ for the overall packing fractions η=0.1 (circles), 0.2 (squares), and 0.34 (triangles). The symbols are the simulation values (Ref. 34); the curves are from the present theory.

retical predictions with Monte Carlo simulation data[34] for the intermolecular site–site radial distribution functions in hard-sphere 8-mers. From Figs. 6 and 7, one can see that the correlation hole between middle segments is more pronounced than that between end segments or between an end segment and a middle segment. While our theory predicts correctly the hole effect at low densities, it is not very accurate for the contact values of the correlations functions involving middle segment as the density increases. A possible improvement of current theory is by introducing the multibody correlation functions in the chain-connectivity excess Helmholtz energy functional. Because of the close connection with the neighboring segments, the middle segments are expected to be more sensitive to multibody correlations.

VI. CONCLUSIONS

Correlation functions play a central role in conventional liquid-state theories.[25] From the correlation functions, thermodynamic properties of a monatomic or polymeric fluid can be calculated from one of three approaches in statistical mechanics: compressibility equation, virial equation, and the energy equation. One long-standing problem in statistical theory of classical fluids is that because the correlation functions are calculated by approximate means, thermodynamic properties from different approaches are often inconsistent. Besides, because calculation of thermodynamic properties involves integration of correlation functions at the entire range of density, practical applications of the liquid-state theories for phase-equilibrium calculations are often severely limited. Density functional theory, on the other hand, is based on approximations for the excess Helmholtz functional that, for a uniform fluid, is essentially identical to an equation of state. While little guidelines are available to derive excess Helmholtz functionals and indeed current applications

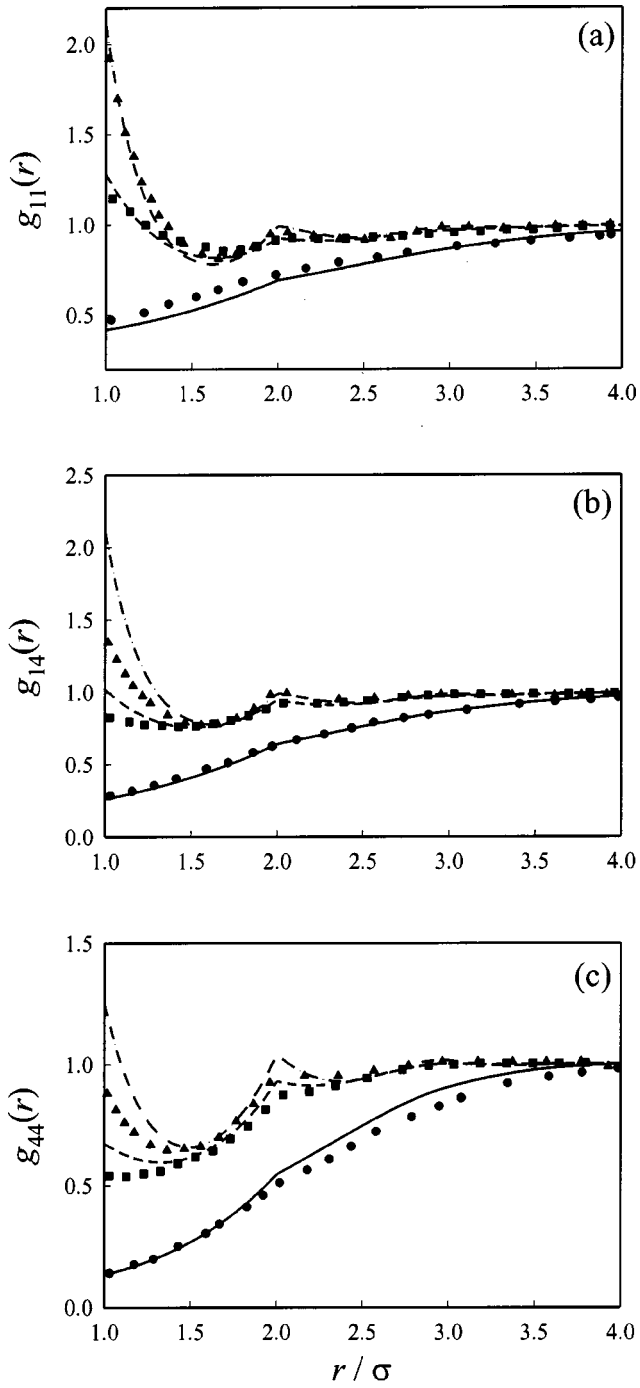

FIG. 7. Intermolecular segment–segment distribution functions of freely jointed hard-sphere 8-mers: (a) $g_{11}(r)$, (b) $g_{14}(r)$, and (c) $g_{44}(r)$ for the overall packing fractions η=0.05 (circles), 0.25 (squares), and 0.35 (triangles). The symbols are the simulation values (Ref. 34); the curves are from the present theory.

are almost exclusively based on the successful results from liquid-state theories, density functional theory provides a systematic framework to extend the established equations of state for applications to inhomogeneous systems and to structural properties. Therefore, density functional theory is a valuable supplementary of conventional liquid-state theories.

In this work, we have extended Percus' test-particle method to predict both intra- and intermolecular correlation functions of bulk polymeric fluids using a density functional theory developed earlier. Applications to freely jointed hard-sphere chains indicate that this method predicts the site–site distribution functions in good agreement with simulation results, especially for the end–end segment radial distribution functions. In comparison with alternative approaches in the literature, the method reported here has the advantages of self-consistency between structural and thermodynamic properties and it is able to predict the nonideal behavior of intramolecular correlation functions.

ACKNOWLEDGMENTS

We gratefully acknowledge the financial support from the University of California Energy Research Institute and the University of California Research and Development Program.

[1] D. Chandler and H. C. Andersen, J. Chem. Phys. **57**, 1930 (1972).
[2] K. S. Schweizer and J. G. Curro, Phys. Rev. Lett. **58**, 246 (1987).
[3] J. G. Curro and K. S. Schweizer, J. Chem. Phys. **87**, 1842 (1987).
[4] K. S. Schweizer and J. G. Curro, Adv. Chem. Phys. **108**, 1 (1997).
[5] D. Chandler and L. R. Pratt, J. Chem. Phys. **65**, 2925 (1976).
[6] L. R. Pratt and D. Chandler, J. Chem. Phys. **66**, 147 (1977).
[7] M. S. Wertheim, J. Stat. Phys. **35**, 19 (1984).
[8] M. S. Wertheim, J. Chem. Phys. **87**, 7323 (1987).
[9] E. Kierlik and M. L. Rosinberg, J. Chem. Phys. **97**, 9222 (1992).
[10] E. Kierlik and M. L. Rosinberg, J. Chem. Phys. **99**, 3950 (1993).
[11] G. Stell and Y. Q. Zhou, J. Chem. Phys. **91**, 3618 (1989).
[12] Y. Q. Zhou and G. Stell, J. Chem. Phys. **96**, 1507 (1992).
[13] Y. Q. Zhou and G. Stell, J. Chem. Phys. **96**, 1504 (1992).
[14] Y. Q. Zhou and G. Stell, J. Chem. Phys. **102**, 8089 (1995).
[15] G. Stell, C. T. Lin, and Y. V. Kalyuzhnyi, J. Chem. Phys. **110**, 5444 (1999).
[16] C. T. Lin, Y. V. Kalyuzhnyi, and G. Stell, J. Chem. Phys. **108**, 6513 (1998).
[17] Y. V. Kalyuzhnyi, C. T. Lin, and G. Stell, J. Chem. Phys. **108**, 6525 (1998).
[18] M. P. Taylor and J. E. G. Lipson, J. Chem. Phys. **102**, 2118 (1995).
[19] H. H. Gan and B. C. Eu, J. Chem. Phys. **103**, 2140 (1995).
[20] Y. C. Chiew, J. Chem. Phys. **93**, 5067 (1990).
[21] Y. C. Chiew, Mol. Phys. **73**, 359 (1991).
[22] Y. P. Tang and B. C. Y. Lu, J. Chem. Phys. **105**, 8262 (1996).
[23] J. Chang and S. I. Sandler, J. Chem. Phys. **102**, 437 (1995).
[24] J. Chang and H. Kim, J. Chem. Phys. **109**, 2579 (1998).
[25] J.-P. Hansen and I. R. McDonald, *Theory of Simple Liquids* (Academic, San Diego, 1986).
[26] A. Yethiraj, H. Fynewever, and S. Chwen-Yang, J. Chem. Phys. **114**, 4323 (2001).
[27] Y.-X. Yu and J. Wu, J. Chem. Phys. **117**, 2368 (2002).
[28] Y.-X. Yu and J. Wu, J. Chem. Phys. **117**, 10156 (2002).
[29] T. Boublik, J. Chem. Phys. **53**, 471 (1970).
[30] G. A. Mansoori, N. F. Carnahan, K. E. Starling, and T. W. Leland, Jr., J. Chem. Phys. **54**, 1523 (1971).
[31] W. G. Chapman, G. Jackson, and K. E. Gubbins, Mol. Phys. **65**, 1057 (1988).
[32] N. F. Carnahan and K. E. Starling, J. Chem. Phys. **51**, 635 (1969).
[33] A. Yethiraj and C. K. Hall, J. Chem. Phys. **93**, 5315 (1990).
[34] A. Yethiraj, C. K. Hall, and K. G. Honnell, J. Chem. Phys. **93**, 4453 (1990).